

^7Be - and ^8B -reaction dynamics at Coulomb barrier energies

M. MAZZOCCO^{1,2}, A. BOIANO³, C. BOIANO⁴, M. LA COMMARA^{3,5},
C. MANEA², C. PARASCANDOLO³, D. PIERROUTSAKOU³, C. SIGNORINI⁶,
E. STRANO^{1,2}, D. TORRESI^{1,2}, H. YAMAGUCHI⁷, D. KAHL⁷,
L. ACOSTA^{8,9}, P. DI MEO³, J.P. FERNANDEZ-GARCIA⁹, T. GLODARIU¹⁰,
J. GREBOSZ¹¹, A. GUGLIELMETTI^{4,12}, N. IMAI^{7,13}, Y. HIRAYAMA¹³,
H. ISHIYAMA¹³, N. IWASA¹⁴, S.C. JEONG^{13,15}, H.M. JIA¹⁶,
N. KEELEY¹⁷, Y.H. KIM¹³, S. KIMURA¹³, S. KUBONO^{7,18}, J.A. LAY^{1,2},
C.J. LIN¹⁶, G. MARQUINEZ-DURAN⁸, I. MARTEL⁸, H. MIYATAKE¹³,
M. MUKAI¹³, T. NAKAO¹⁹, M. NICOLETTO², A. PAKOU²⁰, K. RUSEK²¹,
Y. SAKAGUCHI⁷, A.M. SÁNCHEZ-BENÍTEZ⁸, T. SAVA¹⁰, O. SGOUROS²⁰,
C. STEFANINI^{1,2}, F. SORAMEL^{1,2}, V. SOUKERAS²⁰, E. STILIARIS²²,
L. STROE¹⁰, T. TERANISHI²³, N. TONIOLO⁶, Y. WAKABAYASHI¹⁸,
Y.X. WATANABE¹³, L. YANG¹⁶ and Y.Y. YANG²⁴

- ¹ Dipartimento di Fisica e Astronomia, Università di Padova, Padova, Italy
² INFN, Sezione di Padova, Padova, Italy
³ INFN, Sezione di Napoli, Napoli, Italy
⁴ INFN, Sezione di Milano, Milano, Italy
⁵ Dipartimento di Fisica, Università di Napoli “Federico II”, Napoli, Italy
⁶ INFN - Laboratori Nazionali di Legnaro, Legnaro (PD), Italy
⁷ CNS - The University of Tokyo, RIKEN campus, Wako, Saitama, Japan
⁸ Departamento de Física Aplicada, Universidad de Huelva, Huelva, Spain
⁹ INFN, Sezione di Catania, Catania, Italy
¹⁰ NIPNE, Măgurele, Romania
¹¹ IFJ PAN, Kraków, Poland
¹² Dipartimento di Fisica, Università di Milano, Milano, Italy
¹³ KEK, Tsukuba, Ibaraki, Japan
¹⁴ Department of Physics, Sendai, Miyagi, Japan
¹⁵ Institute for Basic Science, Daejeon, Korea
¹⁶ China Institute of Atomic Energy, Beijing, China
¹⁷ National Centre for Nuclear Research, Otwock, Poland
¹⁸ RIKEN Nishina Center, Wako, Saitama, Japan
¹⁹ Advanced Science Research Center, JAEA, Tokai, Ibaraki, Japan
²⁰ Department of Physics, University of Ioannina, Ioannina, Greece
²¹ Heavy Ion Laboratory, University of Warsaw, Warsaw, Poland
²² Department of Physics, University of Athens, Athens, Greece
²³ Department of Physics, Kyushu University, Hakozaki, Fukuoka, Japan
²⁴ Institute of Modern Physics, Chinese Academy of Sciences, Lanzhou, China

Abstract

We investigated the reaction dynamics induced by the Radioactive Ion Beams ${}^7\text{Be}$ and ${}^8\text{B}$ on a ${}^{208}\text{Pb}$ target at energies around the Coulomb barrier. The two measurements are strongly interconnected, being ${}^7\text{Be}$ ($S_\alpha = 1.586$ MeV) the loosely bound core of the even more exotic ${}^8\text{B}$ ($S_p = 0.1375$ MeV) nucleus. Here we summarize the present status of the data analysis for the measurement of the elastic scattering process for both reactions and the preliminary results for the optical model analysis of the collected data.

1 Introduction

The reaction dynamics induced by light weakly-bound Radioactive Ion Beams (RIBs) at near-barrier energies has attracted the interest of the Nuclear Physics community for the last 20 years at least. The exotic features of several light RIBs together with their extremely weak binding energies (S_p , S_n and S_α typically lower than 1.0 MeV) make these nuclei an ideal playground for the nuclear reaction theory. From an experimental point-of-view, a large enhancement of the reaction cross section at sub-barrier energies has been observed. This enhancement is mostly due to direct processes, such as the 2n-transfer for the 2n-halo nucleus ${}^6\text{He}$ [1–3] and the neutron skin nucleus ${}^8\text{He}$ [4, 5] and, apparently, the breakup process for ${}^8\text{B}$ - [6] and ${}^{11}\text{Li}$ -induced [7, 8] reactions. Contrary to initial expectations, only a marginal enhancement, when recorded, of the fusion cross section at sub-barrier energies has been reported [4, 5]. Several review papers have been published on this topic over the last decade [9–15]

In this contribution we describe the present status of the data analysis for our measurements of the elastic scattering process for the systems ${}^7\text{Be} + {}^{208}\text{Pb}$ and ${}^8\text{B} + {}^{208}\text{Pb}$ at near-barrier energies.

2 The system ${}^7\text{Be} + {}^{208}\text{Pb}$

This reaction was studied at the Laboratori Nazionali di Legnaro (LNL, Italy) of the Istituto Nazionale di Fisica Nucleare (INFN), where a ${}^7\text{Be}$ RIB is routinely delivered by the facility EXOTIC [16, 17]. The ${}^7\text{Be}$ beam for this experiment was obtained starting from a 48.8 MeV ${}^7\text{Li}^{3+}$ primary beam impinging on a 5-cm long gas target filled with 1 bar of H_2 gas cooled down to liquid nitrogen temperature (~ 90 K). In these conditions, a 40.5-MeV ${}^7\text{Be}$ secondary beam with an average intensity $2\text{--}3 \times 10^5$ pps was produced. A second ${}^7\text{Be}$ energy of 37.6 MeV was obtained by means of an approximately $12.5 \mu\text{m}$ thick Al degrader inserted along the beam line right before the main scattering chamber. Finally, a third energy of 42.4 MeV was achieved at the end of the experiment after warming up the target station at room temperature. In all cases the secondary beam purity was as good as 99%.

Charged particles originated by the interaction with a 1 mg/cm^2 ${}^{208}\text{Pb}$ target were detected in the angular ranges $\theta_{lab} = [55^\circ, 84^\circ]$, $[96^\circ, 125^\circ]$ and $[138^\circ, 165^\circ]$ by means of 6 ΔE - E_{res} telescopes of the newly developed detector array EXPADES [18]. The telescopes were displaced in a cylindrical configuration around the target at an average distance of about 111.5 mm.

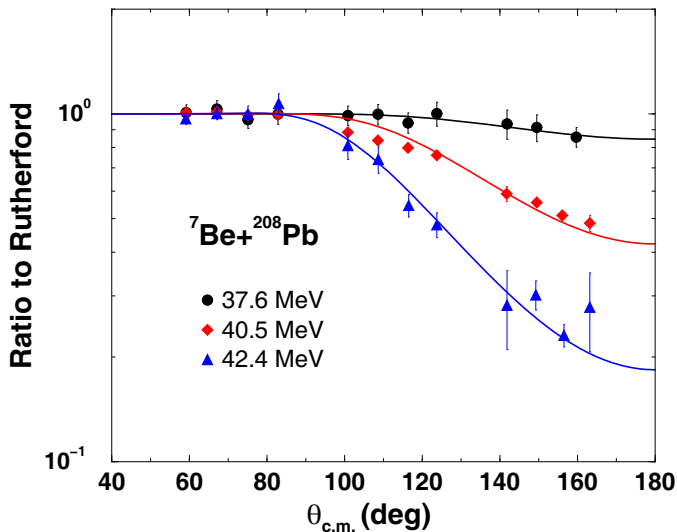


Figure 1: Elastic scattering angular distributions for the system ${}^7\text{Be} + {}^{208}\text{Pb}$ at three bombarding energies. Continuous lines represent the results of an optical model best-fit analysis of the experimental data.

Three modules were located in the left hemisphere and the other three in symmetrical locations of the right hemisphere. Each telescope consisted of a 43-57 and 300 μm thick Double Sided Single Strip Detector (DSSDS) as inner and outer layer, respectively. Each DSSSD had an active area of 62.3 mm \times 62.3 mm and each side was segmented into 32 strips, determining a position resolution of about 2 mm \times 2 mm.

Fig. 1 shows a preliminary evaluation of the elastic scattering angular distributions for the system ${}^7\text{Be} + {}^{208}\text{Pb}$. We can directly appreciate the drop of the differential cross section at backward angles due to the nuclear absorption. To contain statistical fluctuations, at this stage of the analysis, the data were grouped into bins of 8 vertical strips. A better angular resolution should be achieved after completing the sorting procedure of the collected data.

Continuous lines in Fig. 1 are the result of an optical model best fit analysis of the experimental data within the framework of the optical model. The analysis was performed with the SFRESCO subroutine of the main code FRESCO [19] and allowed the extraction of the reaction cross section. The comparison of the reaction cross sections for the system 6, 7Li, ${}^7\text{Be}$ and ${}^8\text{B} + {}^{208}\text{Pb}$ will be presented in the last section of this contribution.

3 The system ${}^8\text{B} + {}^{208}\text{Pb}$

The study of this reaction was carried out at the CRIB (CNS Radioactive Ion Beam) [20,21] facility located in the RIKEN campus at Wako (Japan). A 50 MeV ${}^8\text{B}$ RIB was produced starting from a 66 MeV ${}^6\text{Li}^{3+}$ primary beam impinging on a 8-cm long gas target inflated with ${}^3\text{He}$ gas at a pressure of 1 bar. The outgoing ${}^8\text{B}$ beam had an intensity of 2×10^4 pps and a purity of about 20%, being the ${}^6\text{Li}$ scattered beam, ${}^3\text{He}$ ions recoiling out from the gas target and ${}^7\text{Be}$ the main contaminant beams. However, all these beams had different times of flight (ToF) through the CRIB separator and, by using proper gates in the ToF spectra, it will be possible to discriminate events originating from different components of the cocktail beam.

Charged reaction products arising from the interaction with a 2.2 mg/cm^2 ${}^{208}\text{Pb}$ (evaporated on a $1.5 \mu\text{m}$ thick Mylar backing foil) were detected by means of the six ΔE - E_{res} modules of the already mentioned detector array EXPADES. In this experiment a slightly asymmetric configuration of the telescopes was employed in order to ensure the coverage of the following angular ranges: $\theta_{lab} = [16^\circ, 41^\circ]$, $[55^\circ, 84^\circ]$, $[96^\circ, 125^\circ]$ and $[139^\circ, 164^\circ]$. The average distance between the detectors and the target central position was about 113 mm.

Fig. 2 shows a very preliminary evaluation of the angular distribution for the elastic scattering process in the system ${}^8\text{B} + {}^{208}\text{Pb}$. Only four points were plotted, each one corresponding to the mean location of the four angular ranges covered by the EXPADES array. The experimental data were normalized by using a Monte-Carlo simulation, which took into account the geometry of the detector array and the kinematics of the elastic scattering process. Simulated events were generated according to a pure Rutherford cross section. The ratio between experimental and simulated data was finally set equal to unity in the angular range covered by the detector located at the forward-most angles. In the next months we expect to improve the angular resolution of the elastic scattering differential cross section by performing a detailed strip-by-strip analysis of the gathered data and, if allowed by the collected statistics, to proceed also with a pixel-by-pixel analysis.

Continuous line in Fig. 2 represents the result of an optical model best fit analysis performed with the code FRESKO. This procedure allowed us to extract a first (extremely preliminary) evaluation of the reaction cross section for the system ${}^8\text{B} + {}^{208}\text{Pb}$ at 50 MeV beam energy.

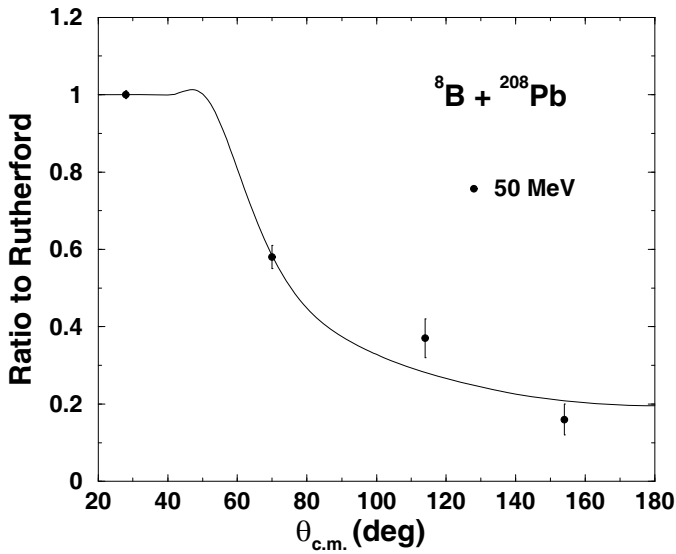


Figure 2: Preliminary elastic scattering angular distribution for the system ${}^8\text{B} + {}^{208}\text{Pb}$ at 50 MeV beam energy. The continuous line is the result of the optical model analysis of the collected data.

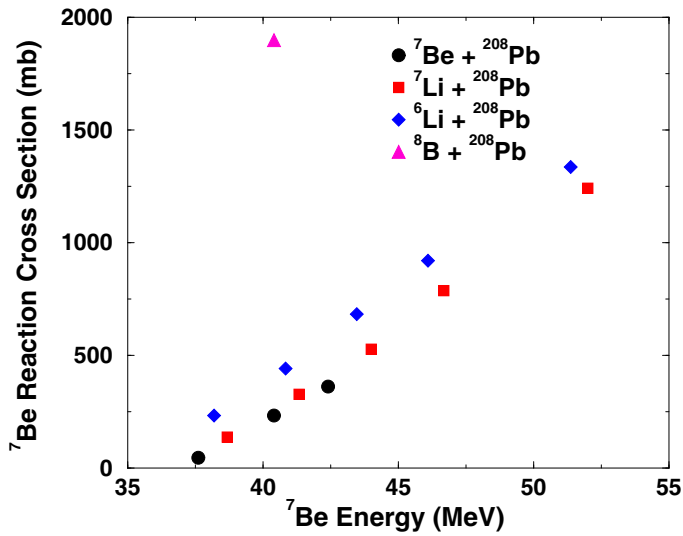


Figure 3: Reaction cross sections for the systems ${}^6,{}^7\text{Li}$, ${}^7\text{Be}$ and ${}^8\text{B} + {}^{208}\text{Pb}$. The data were reduced according to the procedure recommended in Ref. [23] and then normalized to the system ${}^7\text{Be} + {}^{208}\text{Pb}$.

4 Discussion

Fig. 3 illustrates the reaction cross sections for the systems ${}^6,{}^7\text{Li}$ [22], ${}^7\text{Be}$ and ${}^8\text{B} + {}^{208}\text{Pb}$ in the energy range around the Coulomb barrier. The data for the different systems were reduced according to the procedure described in Ref. [23] and then multiplied by the normalization factor of the reaction ${}^7\text{Be} + {}^{208}\text{Pb}$. It is interesting to observe that, according to our preliminary analysis, the ${}^7\text{Be}$ ($S_\alpha = 1.586$ MeV) nucleus exhibits a reactivity rather similar to that of its more bound mirror nucleus ${}^7\text{Li}$ ($S_{\alpha} = 2.467$ MeV), rather than to that of the similarly weakly bound nucleus ${}^6\text{Li}$ ($S_{\alpha} = 1.474$ MeV).

On the other side, it is particularly evident that, even at this very preliminary stage of the data analysis, the reaction induced by the ${}^8\text{B}$ p-halo nucleus ($S_p = 0.1375$ MeV) on the ${}^{208}\text{Pb}$ target has a reaction cross section much larger than those measured for reactions induced by the other weakly-bound projectiles on the same target. This scenario is rather consistent with that observed for reactions induced by the same projectiles on the medium-mass target ${}^{58}\text{Ni}$ [6]. In our case, in an ultimate stage of the data analysis, it should be possible to establish whether the reaction cross section enhancement for the system ${}^8\text{B} + {}^{208}\text{Pb}$ is mainly due to direct channels, such as breakup and/or transfer, or to the fusion process.

Acknowledgments

This work was partially supported by the Italian Minister for Education, University and Research (MIUR) within the project RBFR08P1W2 (FIRB 2008) and the National Science Centre of Poland under contract No. UMO-2014 14 M ST2 00738 (COPIN-INFN Collaboration). The research leading to these results has also received funding from the European Commission, Seventh Framework Programme (FP7 2007-2013) under Grant Agreement n. 600376. J.A.L. is a Marie Curie Piscopia fellow at the University of Padova.

References

- [1] A. Di Pietro *et al.*, Phys. Rev. C **69**, 044613 (2004).
- [2] A. Navin *et al.*, Phys. Rev. C **70**, 044601 (2004).
- [3] R. Raabe *et al.*, Nature **431**, 823 (2004).

- [4] A. Lemasson *et al.*, Phys. Rev. Lett. **103**, 232701 (2009).
- [5] A. Lemasson *et al.*, Phys. Rev. C **82**, 044617 (2010).
- [6] E.F. Aguilera *et al.*, Phys. Rev. C. **79**, 021601(R) (2009).
- [7] M. Cubero *et al.*, Phys. Rev. Lett. **109**, 262701 (2012).
- [8] J.P. Fernandez-Garcia *et al.*, Phys. Rev. Lett. **110**, 142701 (2013).
- [9] L.F. Canto, P.R.S. Gomes, R. Donangelo and M.S. Hussein, Phys. Rep. **424**, 1 (2006).
- [10] J.F. Liang, and C. Signorini, Int. J. Mod. Phys. E **14**, 1121 (2005).
- [11] N. Keeley, R. Raabe, N. Alamanos, and J.L. Sida, Prog. Part. Nucl. Phys. **59**, 579 (2007).
- [12] N. Keeley, N. Alamanos, K.W. Kemper, and K.Rusek, Prog. Part. Nucl. Phys. **63**, 396 (2009).
- [13] M. Mazzocco, Int. J. Mod. Phys. E **19**, 977 (2010).
- [14] N. Keeley, K.W. Kemper and K. Rusek, Eur. Phys. J. A **50**, 145 (2014).
- [15] L.F. Canto, P.R.S. Gomes, R. Donangelo, J. Lubian and M.S. Hussein, Phys. Rep. **596**, 1 (2006).
- [16] F. Farinon *et al.*, Nucl. Instrum. Meth. B **266**, 4097 (2008).
- [17] M. Mazzocco *et al.*, Nucl. Instrum. Meth. B **317**, 223 (2013).
- [18] E. Strano *et al.*, Nucl. Instr. and Meth. B **317** (2013) 657.
- [19] I.J. Thompson, Comput. Phys. Rep. **2**, 167 (1988).
- [20] Y. Yanagisawa *et al.*, Nucl. Instr. and Meth. A **539** (2005) 74.
- [21] H. Yamaguchi *et al.*, Nucl. Instr. and Meth. A **589** (2008) 150.
- [22] N. Keeley *et al.*, Nucl. Phys. A **571** (1994) 326.
- [23] P.R.S. Gomes, J. Lubian, I. Padron, R.M. Anjos, Phys. Rev. C **71** (2005) 017601.